Isostructural $[Au_6Pd_6(Pd_{6-x}Ni_x)Ni_{20}(CO)_{44}]^{6-}$ and $[Au_6Ni_{32}(CO)_{44}]^{6-}$ Clusters Containing Corresponding Nonstoichiometric $Au_6Pd_6(Pd_{6-x}Ni_x)Ni_{20}$ and Stoichiometric Au_6Ni_{32} Nanosized Cores: Substitutional Pd/Ni Crystal Disorder (Coloring Problem) at Only Six Specific Nonadjacent Pseudoequivalent Metal Sites in the 38-Atom Trimetallic Close-Packed Framework

Nguyet T. Tran,[1a] Masaki Kawano,[1a] Douglas R. Powell,[1a] Randy K. Hayashi,[1a] Charles F. Campana,[1b] and Lawrence F. Dahl*,[1a]

Contribution from the Department of Chemistry, University of Wisconsin−Madison, Madison, Wisconsin 53706, and Bruker Analytical X-ray Systems, Incorporated, 6300 Enterprise Lane, Madison, Wisconsin 53719

Received July 27, 1998. Revised Manuscript Received January 29, 1999

Abstract: Efforts to obtain large trimetallic Au−Pd−Ni carbonyl clusters have given rise to the first reported high-nuclearity trimetallic carbonyl cluster $[Au_6Pd_6(Pd_{6-x}Ni_x)Ni_{20}(CO)_{44}]^{6-}$ (**1**). The centrosymmetric architecture of its 38-atom core ideally consists of the hcp stacking of two inner $Au_3M_3Ni_6$ and two outer Pd_3 layers along with two Pd_3-capped and six $AuNi_2$-capped Ni atoms. The resulting octahedral-like Au_6 kernel is antiprismatically capped on opposite triangular faces by the two Pd_3 triangles. The microscopic nature of its nonstoichiometric composition was unequivocally established from complete X-ray diffraction analyses via a SMART CCD system of seven crystals of its $[PPh_4]^+$ salt from different samples. A substitutional Pd/Ni crystal disorder was found at only six specific nonadjacent atomic M sites (three crystallographically independent); for the *composite* six-site crystal disorder of the $(6 − x)$ Pd/x Ni atoms, x was determined for the seven crystals to range from 2.1 (65% Pd, 35% Ni) to 5.5 (8% Pd, 92% Ni). The overall geometry of **1** including the 44 CO ligands (in the crystal-averaged unit cell) ideally has trigonal $D_{3d}(\bar{3}2/m)$ symmetry. A structure/bonding analysis as to why this particular Pd/Ni substitutional crystal disorder is found in **1** provides a striking illustration that the occurrence of a bimetallic substitutional crystal disorder at only certain crystallographic sites (coloring problem) in a *heterometallic carbonyl cluster* is critically dependent upon the extent of dissimilarity in the *composite* relative bond-energy effects of metal−metal/metal−CO interactions. **1** was obtained as a major product (35−40% yields) from reactions of $[Ni_6(CO)_{12}]^{2-}$ with $Pd(OAc)_2/Au(PPh_3)Cl$ mixtures in DMSO. Our desire to obtain the hypothetical isostructrual $[Au_6Ni_{32}(CO)_{44}]^{6-}$ (**2**), in which all Pd atoms are replaced with Ni ones, led to the designed synthesis and structural determination of **2**, which in turn provided an "operational test" of our "coloring-problem" analysis of **1**. The maximum metal-core diameters in **1** and **2** are ca. 1.1 nm parallel and 0.8 nm perpendicular to the principal 3-fold axis.

Introduction

One highly active area in metal cluster chemistry during the last two decades has involved the preparation of mixed transition metal−gold clusters and examination of their physical-chemical properties.[2] A large number of cationic transition metal−gold clusters have been prepared by Pignolet and co-workers[3] from reactions of $Au(PPh_3)NO_3$ with transition metal phosphine complexes containing a group VIII (8−10) metal (with the notable exception of Ni). Incorporation of gold into catalytically active transition metal clusters usually gives rise to significant

increases in their activity and selectivity.[4] Pignolet and co-workers[5] have also shown from extensive studies that phosphine-stabilized Pt−Au and Pd−Au clusters are very active homogeneous catalysts for the H_2/D_2 equilibrium reaction and $D_2(g)-H_2O(l)$ isotope exchange in solution. In addition, they observed

(1) (a) UW−Madison. (b) Bruker AXS, Inc.

(2) (a) Salter, J. D. Cluster Complexes between Transition Elements and Copper, Silver, and Gold. In *Comprehensive Organometallic Chemistry II*; Abel, E. W., Stone, F. G. A., Wilkinson, G., Eds.; Elsevier Science Inc.: Tarrytown, NY, 1995; Vol. 10, Chapter 5, pp 255−322. (b) Jones, P. G. *Gold Bull.* **1986**, *19*, 46 and references therein; **1983**, *16*, 114 and references therein. (c) Braunstein, P.; Rosé, J. *Gold Bull.* **1985**, *18*, 17 and references therein. (d) Hall, K. P.; Mingos, D. M. P. *Prog. Inorg. Chem.* **1984**, *32*, 237 and references therein.

(3) (a) Mueting, A. M.; Bos, W.; Alexander, B. D.; Boyle, P. D.; Casalnuovo, J. A.; Balaban, S.; Ito, L. N.; Johnson, S. M.; Pignolet, L. H. *New J. Chem.* **1988**, *12*, 505 and references therein. (b) Pignolet, L. H.; Aubart, M. A.; Craighead, K. L.; Gould, R. A. T.; Krogstad, D. A.; Wiley, J. S. *Coord. Chem. Rev.* **1995**, *143*, 219 and references therein. (c) Krogstad, D. A.; Konze, W. V.; Pignolet, L. H. *Inorg. Chem.* **1996**, *35*, 6763 and references therein.

(4) (a) Sinfelt, J. H. *Bimetallic Catalysts*; Wiley: New York, 1983; Chapters 1 and 2. (b) Wacks, I. E. *Gold Bull.* **1983**, *16*, 98. (c) Schwank, J. *Gold Bull.* **1985**, *18*, 1 and references therein. (d) Alexander, B. D.; Gomez-Sal, M. P.; Gannon, P. R.; Blaine, C. A.; Boyle, P. D.; Mueting, A. M.; Pignolet, L. H. *Inorg. Chem.* **1988**, *27*, 3301 and references therein. (e) Braunstein, P.; Rosé, J. In *Stereochemistry of Organometallic and Inorganic Compounds*; Bernal, I., Ed.; Elsevier: Tarrytown, NY, 1998; Vol. 3. (f) Ichikawa, M. *Adv. Catal.* **1992**, *38*, 283 and references therein. (g) *Catalysis by Di- and Polynuclear Metal Cluster Complexes*; Adams, R. D., Cotton, F. A., Eds.; Wiley-VCH: New York, 1998; pp 1−555.

that these Pt−Au clusters have similar reactivities when deposited on silica and alumina supports.[5c] The colloidal bimetallic cluster Pd/Au(4/1),[6a] which has the surface layer entirely composed of palladium atoms and a core composed of gold atoms, is one of the most active catalysts for the selective partial hydrogenation of 1,3-cyclooctadiene to cyclooctene. This area also has particular relevance to widespread studies over the last 10 years on the preparation, characterization, and application to catalysis of polymer- or ligand-stabilized bimetallic nanoparticles containing gold.[6b]

The preparation and stereophysical/theoretical investigation of the pseudo-T_d $[Au_6Ni_{12}(CO)_{24}]^{2-}$ cluster (**3**) were previously reported.[7] This research was motivated by the fact that there had been no prior report of any discrete gold−nickel compound containing direct Au−Ni connectivities. The unique molecular geometry of this high-nuclearity metal carbonyl cluster (arbitrarily defined to have at least 10 metal-core atoms that possess direct metal−metal bonding interactions) may be envisioned as five face-fused octahedra resulting from the antiprismatic linkage of four triangular $Ni_3(CO)_3(\mu_2\text{-}CO)_3$ ligands to four alternate triangular faces of a central Au_6 octahedron. Because this air-unstable cluster was obtained only in low yields, its chemical behavior was not investigated.

Subsequent research in our laboratories has given rise to unprecedented high-nuclearity Pd−Ni carbonyl clusters.[8,9] These bimetallic clusters are of particular interest because (1) palladium, in elemental or combined form, is widely utilized in homogeneous/heterogeneous catalysis,[4,5,10] (2) $PdNi_x$ alloys encaged in NaY zeolite are more selective in promoting CO hydrogenation compared with monometallic Pd/NaY and Ni/NaY samples and their physical mixtures,[11] (3) both experimental/theoretical studies[12] on Pd films supported over Ni(111) surfaces have shown that Pd atoms are electronically perturbed and that this perturbation alters their catalytic properties (e.g., a striking catalytic efficiency toward hydrogenation of butadiene is

observed), and (4) a theoretical examination[13] of the electronic properties of Pt, Pd, and Ni in bimetallic surfaces revealed a very good correlation between electronic and physical/chemical properties induced by bimetallic bonding (e.g., bimetallic bonding was shown to deactivate the group X metals toward CO chemisorption). Consequently, we decided to investigate whether large Au−Pd−Ni carbonyl clusters could be isolated in sufficient yields to permit their use as precursors to form possible tailored trimetallic catalysts.

We now report the preparation, structure/bonding analysis, and physical properties of the remarkable $[Au_6Pd_6(Pd_{6-x}Ni_x)Ni_{20}(CO)_{44}]^{6-}$ hexaanion (**1**) as the $[PPh_4]^+$ salt. To our knowledge, **1** is the first crystallographically determined example of a *high-nuclearity trimetallic carbonyl cluster*. This nonstoichiometric compound was obtained as a major product (35−40% yields) from reactions of $[Ni_6(CO)_{12}]^{2-}$ with $Pd(OAc)_2$/Au(PPh$_3$)Cl mixtures in DMSO at room temperature. The microscopic nature of its nonstoichiometric composition (vide infra) was unambiguously established from complete X-ray crystallographic analyses of *seven* crystals from different samples via a SMART CCD area detector diffractometry system. Herein are given the crystallographic results for two different crystals, A and B. The compound was also characterized by elemental analysis and by IR, ^{1}H NMR, and electrochemical measurements.

Noteworthy is that the formation of **1** necessitates Au−PPh$_3$ bond cleavage in the Au(PPh$_3$)Cl precursor, which likewise is required for the preparation of the $[Au_6Ni_{12}(CO)_{24}]^{2-}$ dianion (**3**)[7] but otherwise is not observed in countless metal cluster reactions involving Au(PPh$_3$)X reagents (X = halide, NO$_3$). This nonstoichiometric trimetallic carbonyl cluster is also of special interest in that a qualitative structure/bonding examination provides a rational explanation as to why Pd/Ni substitutional crystal disorder (coloring problem) occurs at only the six nonadjacent atomic sites that are symmetry-related under assumed $D_{3d}(\bar{3}2/m)$ symmetry (vide infra). Our subsequent hypothesis that all Pd sites in **1** can be formally replaced by Ni ones to give the (then unknown) isostructural $[Au_6Ni_{32}(CO)_{44}]^{6-}$ hexaanion (**2**) was fulfilled: A designed preparative reaction led to the successful isolation/crystallization and an X-ray diffraction study of **2**. A geometrical comparison between **1** and **2** has provided an "operational test" for our prior analysis of the microscopic nature of the Pd/Ni substitutional crystal disorder found in **1**. This nonstoichiometric trimetallic cluster thereby provides a striking example that the occurrence of a "coloring problem" at only specific crystallographic metal-core sites in a *heterometallic carbonyl cluster* must be a consequence of the degree of dissimilarity in the composite relative strengths of both metal−metal and metal−CO bonding interactions. Details of this work are presented herein.

Experimental Section

Materials and Techniques. All reactions including sample transfers and manipulations were performed under an atmosphere of dry nitrogen with standard Schlenk techniques on a preparative vacuum line. The $[NMe_4]^+$ salt of the $[Ni_6(CO)_{12}]^{2-}$ dianion was prepared by a modification of the general method of Longoni, Chini, and Cavalieri.[14] Other chemicals were purchased from STREM and used without further purification. The following solvents were freshly distilled under nitrogen from the indicated appropriate drying agents immediately prior to use: methanol (Mg); tetrahydrofuran (K/benzophenone); acetone (CaSO$_4$);

(5) (a) Pignolet, L. H.; Aubart, M. A.; Craighead, K. L.; Gould, R. A. T.; Krogstad, D. A.; Wiley, J. S. *Coord. Chem. Rev.* **1995**, *143*, 219 and references therein. (b) Rubenstein, L. I.; Pignolet, L. H. *Inorg. Chem.* **1996**, *35*, 6755. (c) Graf, I. V. G.; Bacon, J. W.; Consugar, M. B.; Curley, M. E.; Ito, L. N.; Pignolet, L. H. *Inorg. Chem.* **1996**, *35*, 689.

(6) (a) Harada, M.; Asakura, K.; Toshima, N. *J. Phys. Chem.* **1993**, *97*, 5103. (b) Toshima, N.; Yonezawa, T. *New J. Chem.* **1998**, *22*, 1179 and references therein.

(7) (a) Whoolery, A. J.; Dahl, L. F. *J. Am. Chem. Soc.* **1991**, *113*, 6683. (b) Johnson, A. J. W.; Spencer, B.; Dahl, L. F. *Inorg. Chim. Acta* **1994**, *227*, 269.

(8) (a) Kawano, M.; Bacon, J. W.; Campana, C. F.; Dahl, L. F. *J. Am. Chem. Soc.* **1996**, *118*, 7869. (b) Kawano, M.; Bacon, J. W.; Campana, C. F.; Winger, B. E.; Dudek, J. D.; Sirchio, S. A.; Scruggs, S. L.; Williams, J. M.; Dahl, L. F. Paper in preparation. (c) Tran, N. T.; Kawano, M.; Hayashi, R. K.; Dahl, L. F. Paper in preparation.

(9) Two new cocrystallized Pt−Ni carbonyl clusters, $[Pt_4Ni_{36}(CO)_{45}]^{6-}$ and $[Pt_4Ni_{37}(CO)_{46}]^{6-}$ with each containing a Pt$_4$ tetrahedron encapsulated in an incomplete tetrahedron of nickel atoms, were recently reported (Demartin, F.; Femoni, C.; Iapalucci, M. C.; Longoni, G.; Macchi, P. *Angew. Chem., Int. Ed. Engl.* **1999**, *38*, 531).

(10) (a) Malleron, J.-L.; Fiaud, J.-C.; Legros, J. Y. *Handbook of Palladium Catalysed Organic Reactions*; Academic Press: San Diego, CA, 1997. (b) Malleron, J.-L.; Juin, A. In *Database of Palladium Chemistry*; Academic Press: San Diego, CA, 1997. (c) Sachtler, W. M. H.; Stakheev, A. Yu. *Catal. Today* **1992**, *12*, 283 and references therein. (d) Zhang, Z.; Xu, L.; Sachtler, W. M. H. *J. Catal.* **1991**, *131*, 502. (e) Sinfelt, J. H. *Acc. Chem. Res.* **1987**, *20*, 134. (f) Gallezot, P. In *Metal Clusters*; Moskovits, M., Ed.; J. Wiley: New York, 1986; pp 219−247. (g) Gates, B. C. *Catalytic Chemistry*; J. Wiley: New York, 1992. (h) Moiseev, I. I.; Vargaftik, M. N. *New J. Chem.* **1998**, *22*, 1217.

(11) (a) Feeley, J. S.; Stakheev, A. Yu; Cavalcanti, A. P.; Sachtler, W. M. H. *J. Catal.* **1992**, *136*, 182. (b) Feeley, J. S.; Sachtler, W. M. H. *J. Catal.* **1991**, *131*, 573.

(12) (a) Bertolini, J. C.; Miegge, P.; Hermann, P.; Rousset, J. L.; Tardy, B. *Surf. Sci.* **1995**, *331*, 651. (b) Hermann, P.; Tardy, B.; Simon, D.; Guigner, J. M.; Bigot, B.; Bertolini, J. C. *Surf. Sci.* **1994**, *307*, 422. (c) Hermann, P.; Simon, D.; Bigot, B. *Surf. Sci.* **1996**, *350*, 301.

(13) Rodriguez, J. A. *Surf. Sci.* **1996**, *345*, 347.

(14) (a) Calabrese, J. C.; Dahl, L. F.; Cavalieri, A.; Chini, P.; Longoni, G.; Martinengo, S. *J. Am. Chem. Soc.* **1974**, *96*, 2616. (b) Longoni, G.; Chini, P.; Cavalieri, A. *Inorg. Chem.* **1976**, *15*, 3025. (c) Ceriotti, A.; Longoni, G.; Piva, G. *Inorg. Synth.* **1989**, *26*, 312.

[Au₆Pd₆(Pd₆₋ₓNiₓ)Ni₂₀(CO)₄₄]⁶⁻ and [Au₆Ni₃₂(CO)₄₄]⁶⁻

J. Am. Chem. Soc., Vol. 121, No. 25, 1999 5947

acetonitrile (CaH₂); diisopropyl ether (K/benzophenone). DMSO was thoroughly purged with nitrogen before use.

All ¹H NMR and ¹³C NMR spectra were recorded on a Bruker AM-500 spectrometer. All NMR samples were prepared via a freeze–pump–thaw technique. Infrared spectra were recorded on a Nicolet 740 FT-IR spectrophotometer with nitrogen-purged CaF₂ cells. Electrochemical measurements were performed with a Bioanalytical Systems BAS-100 Electrochemical Analyzer with the electrochemical cell enclosed in a nitrogen-filled atmosphere glovebox. The cell consisted of a platinum disk working electrode and a coiled platinum wire counter electrode. The reference electrode was a porous Vycor-tipped aqueous saturated calomel electrode separated from the test solution by a salt bridge filled with a 0.1 M [n-Bu₄N]⁺[PF₆]⁻ in THF solution. The same supporting electrolyte was used in the salt bridge.

Synthesis of [Au₆Pd₆(Pd₆₋ₓNiₓ)Ni₂₀(CO)₄₄]⁶⁻ (1) as the [PPh₄]⁺ Salt. (a) Reactions of Pd(OAc)₂, Au(PPh₃)Cl, and [Ni₆(CO)₁₂]²⁻. In a typical reaction, a solution of Au(PPh₃)Cl (0.07 g; 0.15 mmol) in 10 mL of DMSO was quickly added to a stirred solution of Pd(OAc)₂ (0.10 g; 0.45 mmol) in 10 mL of DMSO. This mixture was then added dropwise over 20 min into a solution of [Me₄N]⁺₂[Ni₆(CO)₁₂]²⁻ (0.25 g; 0.30 mmol) in 10 mL of DMSO. The reaction mixture, which turned from dark cherry red to dark brown, was stirred for 2 days at room temperature. PPh₄Br (2.5 g) in 10 mL of MeOH was then added into the reaction solution. Slow addition of water to an ice-cooled reaction solution gave a dark brown precipitate, which was filtered off and washed with methanol followed by THF. The solid was extracted with acetone and then with acetonitrile. Black opaque prismatic crystals (including crystal A) of the title compound were obtained (0.06–0.07 g) from the acetonitrile extract layered with diisopropyl ether. Yields of 35–40% are based on Au(PPh₃)Cl. The dark-brown air-unstable **1** is soluble in acetonitrile and DMSO.

(b) Reactions of Pd(OAc)₂/Ni(OAc)₂, and Au(PPh₃)Cl with [Ni₆(CO)₁₂]²⁻. A solution of Au(PPh₃)Cl (0.07 g; 0.15 mmol) in 10 mL of DMSO was quickly added to a stirred solution of Pd(OAc)₂ (0.05 g; 0.20 mmol) and Ni(OAc)₂·4H₂O (0.05 g; 0.20 mmol) in 10 mL of DMSO. This mixture was then added dropwise over 20 min into a solution of [Me₄N]⁺₂[Ni₆(CO)₁₂]²⁻ (0.17 g; 0.20 mmol) in 10 mL of DMSO. The reaction mixture, which turned from dark cherry red to dark brown, was stirred for 2 days at room temperature. The reaction was then worked up in the same way as the above-mentioned reaction. The acetone extract gave 0.13 g of **1** (yield ca. 73% based on Au(PPh₃)Cl), from which crystal B was obtained. The acetonitrile extract gave 0.04 g of **1** (yield ca. 20% based on Au(PPh₃)Cl).

Elemental Analysis and Spectroscopic/Electrochemical Characterization of [Au₆Pd₆(Pd₆₋ₓNiₓ)Ni₂₀(CO)₄₄]⁶⁻ (1) as the [PPh₄]⁺ Salt. An elemental analysis (Desert Analytics, Tucson, AZ) was performed on crystals of the same sample from which crystal A was obtained and crystallographically analyzed. Calculated values based upon crystal A are for [PPh₄]⁺₆[Au₆Pd₆(Pd₆₋ₓNiₓ)Ni₂₀(CO)₄₄]⁶⁻·4.72(MeCN)·(i-Pr₂O); $x = 2.92$ (FW = 7058.06). Calculated (found): Au, 16.74 (16.45); Pd, 13.69 (13.18); Ni, 19.06 (20.44); C, 34.61 (34.04); H, 2.12 (2.07); N, 0.94 (0.98). This comparison does *not* imply that all crystals in that sample would be expected to have the same fixed nonstoichiometric composition (i.e., the same composite Pd/Ni substitutional disorder denoted by x) as that in crystal A. Nevertheless, the agreement between corresponding calculated and observed percentages is reasonably good for each element.

An IR spectrum of **1** in acetonitrile exhibited several carbonyl absorption bands at 2013 (s), 1990 (m), and 1884 (vs) cm⁻¹. A ¹H NMR spectrum (500 MHz, CD₃CN at 23 °C) showed a multiplet at 7.6–8.0 ppm for the phenyl protons of [PPh₄]⁺, a septet at 3.6 ppm, and a doublet at 1.05 ppm with $J = 6.5$ Hz for protons of the solvated diisopropyl ether in crystals. No high-field signals corresponding to hydride-like atoms were detected; moreover, no paramagnetic shifts of the phenyl proton resonances were observed. A ¹³C NMR spectrum (126 MHz, CD₃CN) gave signals corresponding to only the [PPh₄]⁺ counterions; resonances characteristic of the carbonyl ligands were not detected either at room temperature or at −30 °C.

A CV with a 50 mV/s scan rate of **1** in acetonitrile (0.1 M TBAPF₆ as supporting electrolyte) at a platinum disk working electrode displayed one irreversible oxidation wave at ca. 1.35 V, one irreversible reduction

wave at ca. −1.93 V, and one quasi-reversible redox wave at +0.14 and −0.46 V (vs SCE).

Synthesis, Isolation, and Characterization of [Au₆Ni₃₂(CO)₄₄]⁶⁻ (2) as the [PPh₄]⁺ Salt. In a typical reaction, a solution of Au(PPh₃)-Cl (0.07 g; 0.15 mmol) in 10 mL of DMSO was quickly added to a stirred solution of Ni(OAc)₂ (0.11 g; 0.45 mmol) in 10 mL of DMSO. This mixture was then added dropwise over 20 min into a solution of [NMe₄]⁺₂[Ni₆(CO)₁₂]²⁻ (0.25 g; 0.30 mmol) in 10 mL of DMSO. The reaction mixture, which turned from dark cherry red to dark brown, was stirred for 2 days at room temperature. PPh₄Br (2.5 g) in 10 mL of MeOH was added into the solution. Slow addition of water to the ice-cooled solution gave a dark brown precipitate, which was filtered and washed with methanol and then exclusively with THF. An acetone extract produced **2** together with two other Au–Ni carbonyl clusters. Attempts to date to separate **2** from the other two products in solution have not been successful. However, a slow vapor diffusion of diisopropyl ether into the concentrated acetone extract gave rise to a few crystals of each of the three products. The Pasteur technique[15] was utilized to separate physically by manual sorting crystals of **2** for both X-ray diffraction and IR measurements. An IR spectrum (MeCN) of **2** exhibited carbonyl bands at 2013 (s), 1990 (m), and 1880 (vs) cm⁻¹ and a relatively weak shoulder at 1857 cm⁻¹. The dark-brown air-unstable **2** is soluble in acetone, acetonitrile, and DMSO.

X-ray Crystallographic Analyses. (a) General Procedures. Intensity data for each compound were collected via a SMART CCD area detector mounted on a Bruker P4 diffractometer with graphite-monochromated Mo Kα radiation from a sealed-tube generator.

(b) [PPh₄]⁺₆[Au₆Pd₆(Pd₆₋ₓNiₓ)Ni₂₀(CO)₄₄]⁶⁻. Crystallographic data are given for two crystals A and B selected from different samples. Black opaque prismatic crystals from each sample were obtained from a slow diffusion of diisopropyl ether into a concentrated solution of **1** in MeCN.

(1) Crystal A: [PPh₄]⁺₆[Au₆Pd₆(Pd₆₋ₓNiₓ)Ni₂₀(CO)₄₄]⁶⁻·4.72(MeCN)· (i-Pr₂O), $x = 2.92$; triclinic, P1̄; $a = 18.2816(3)$ Å, $b = 18.3972(4)$ Å, $c = 18.8929(4)$ Å, $\alpha = 72.871(2)°$, $\beta = 66.233(2)°$, $\gamma = 68.891(2)°$, $V = 5341.45(18)$ Å³, $Z = 1$, d(calcd) = 2.194 Mg/m³. A sphere of 32 601 data was collected at 133(2) K via 0.3° φ scans over a 2θ range 3.08–52.00°; an empirical absorption correction was applied. Structural determination was obtained by direct methods. Anisotropic least-squares refinement (1363 parameters/22 restraints for solvent) on 18 254 independent merged reflections ($R_{int} = 0.032$) converged at $\omega R_2(F^2) = 0.087$ for all data; $R_1(F) = 0.032$ for 17 099 observed data ($I > 2\sigma(I)$).

(2) Crystal B: [PPh₄]⁺₆[Au₆Pd₆(Pd₆₋ₓNiₓ)Ni₂₀(CO)₄₄]⁶⁻·3.18(MeCN)· 1.29(i-Pr₂O), $x = 2.10$; triclinic, P1̄; $a = 18.3769(4)$ Å, $b = 18.4927(4)$ Å, $c = 19.0021(4)$ Å, $\alpha = 72.807(1)°$, $\beta = 66.166(1)°$, $\gamma = 68.854(1)°$, $V = 5423.6(2)$ Å³, $Z = 1$, d(calcd) = 2.226 Mg/m³. A sphere of 35 749 data was collected at 148(2) K via 0.3° φ scans over a 2θ range 3.66–50.00°; an empirical absorption correction was applied. Structural determination was obtained by direct methods. Anisotropic least-squares refinement (1317 parameters/19 restraints) on 18 931 independent merged reflections ($R_{int} = 0.054$) converged at $\omega R_2(F^2) = 0.113$; $R_1(F) = 0.044$ for 12 730 observed data ($I > 2\sigma(I)$).

(c) [PPh₄]⁺₆[Au₆Ni₃₂(CO)₄₄]⁶⁻·4.5MeCN: triclinic, P1̄; $a = 18.0987(16)$ Å, $b = 18.3287(16)$ Å, $c = 18.7028(16)$ Å, $\alpha = 73.610(2)°$, $\beta = 65.903(2)°$, $\gamma = 68.668(2)°$, $V = 5209.9(8)$ Å³, $Z = 1$, d(calcd) = 2.076 Mg/m³. A sphere of 69 376 data was collected at 138(2) K via 0.4° φ scans over a 2θ range of 3.14–56.64°; an empirical absorption correction was applied. Structural determination was obtained by direct methods. Anisotropic least-squares refinement (1300 parameters/15 restraints for solvent) on 24 194 independent merged reflections ($R_{int} = 0.062$) converged at $\omega R_2(F^2) = 0.124$ for all data; $R_1(F) = 0.046$ for 15 533 observed data ($I > 2\sigma(I)$).

Further details of the crystallographic analyses and tables of atomic coordinates and displacement ellipsoids, distances, and angles for each compound are presented elsewhere as Supporting Information.

Results and Discussion

Structural Features of [Au₆Pd₆(Pd₆₋ₓNiₓ)Ni₂₀(CO)₄₄]⁶⁻ (1). The entire geometry of **1** possesses crystallographic $C_i(\bar{1})$

(15) (a) Pasteur, L. *Ann. Chim. Phys.* **1848**, *24*, 442. (b) Kauffman, G. B.; Myers, R. D. *J. Chem. Educ.* **1975**, *52*, 777.
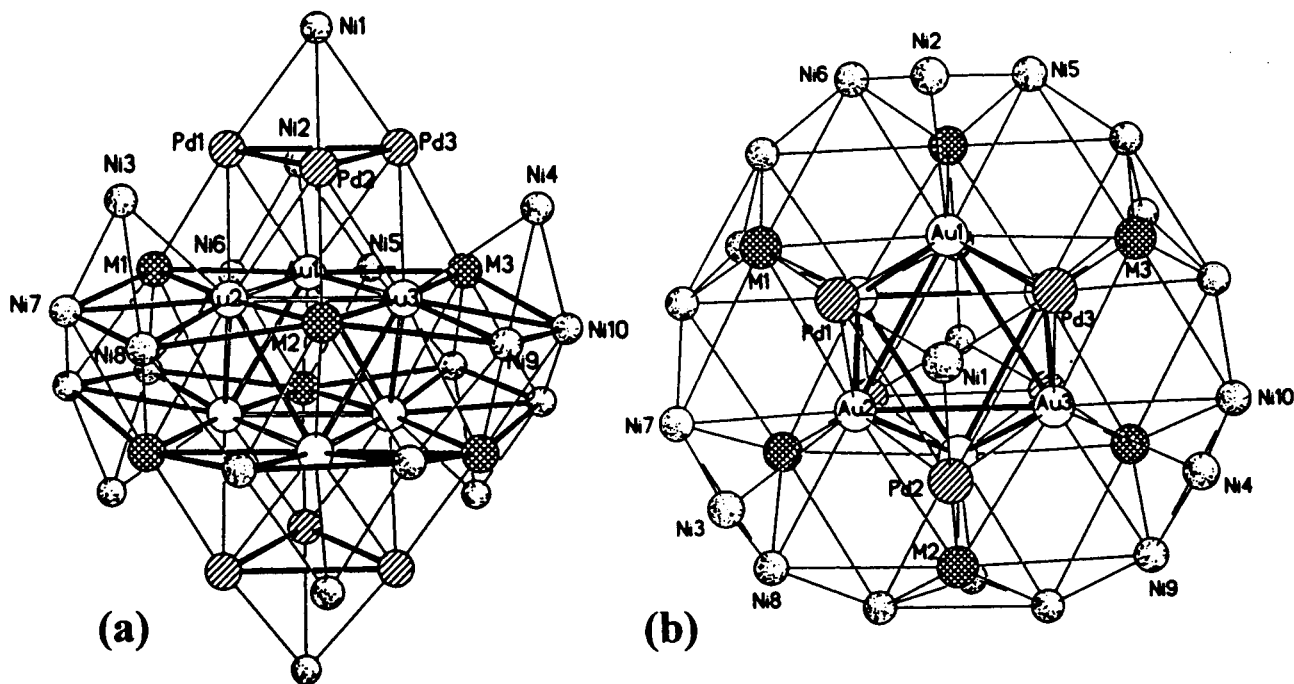
Figure 1. Side view (a) and top view (b) of the 38-atom trimetallic core in the nonstoichiometric $[Au_6Pd_6(Pd_{6-x}Ni_x)Ni_{20}(CO)_{44}]^{6-}$ (**1**). This nanosized core of crystallographic $C_i(\bar{1})$ symmetry ideally consists of a four-layer hcp stacking of two inner $Au_3M_3Ni_6$ and two outer Pd_3 layers along with two Pd_3-capped and six $AuNi_2$-capped Ni atoms. The resulting octahedral-like Au_6 kernel is antiprismatically capped on opposite triangular faces by the two Pd_3 triangles. Substitutional Pd/Ni crystal disorders occur only at the six atomic M sites; for the *composite* six-site Pd_{6-x}/Ni_x crystal disorder, x was crystallographically determined for seven crystals to range from 2.1 to 5.5. Based upon the six *individual* crystal-disordered M sites (three independent) having symmetry-equivalent Pd/Ni occupancies, the overall metal-core geometry ideally has trigonal $D_{3d}(\bar{3}2/m)$ symmetry.

symmetry such that half of this hexaanion is independent. Its 38-atom trimetallic architecture (Figure 1) may be ideally described as a hcp four-layer arrangement of 30 atoms composed of two inner corner-truncated ν_4 triangular $Au_3M_3Ni_6$ layers and two outer triangular Pd_3 layers. Each identical inner layer has a central pseudoequilateral Au_3 triangle that is symmetrically linked along its three edges to three atomic sites (labeled M); each of these M sites has a crystallographically independent substitutional Pd_{1-a}/Ni_a crystal disorder. In turn, the pseudoequilateral Au_3M_3 triangle is joined along each of its three M$-$Au$-$M edges to two connected Ni atoms that are aligned such that each Ni atom is bridge-linked to a Au$-$M half-edge. The centrosymmetric stacking of the resulting two inner Au_3M_3-Ni_6 layers and the two outer triangular Pd_3 layers gives rise to an inner pseudooctahedral Au_6 kernel that is joined on opposite triangular faces to the two Pd_3 triangles by trigonal-antiprismatic capping. The ensuing $Pd_3-Au_3-Au_3-Pd_3$ part of this four-layer 30-atom $Au_6Pd_6M_6Ni_{12}$ fragment corresponds to a face-sharing trioctahedron. Eight Ni atoms cap both outer triangular Pd_3 faces and the outer six $AuNi_2$ triangles within the two 12-atom Au_3M_3-Ni_6 inner layers. Each Au atom has bonding connectivities to 12 atomic sites corresponding to a localized hcp environment.

Crystallographic least-squares refinement of the occupancy factors for the three independent crystal-disordered M sites (labeled M(n); $n = 1, 2, 3$) gave *individual* Pd_{1-a}/Ni_a occupancies of 0.48(1)/0.52(1), 0.49(1)/0.51(1), and 0.58(1)/0.42(1) for crystal A and 0.72(1)/0.28(1), 0.63(1)/0.37(1), and 0.60(1)/0.40-(1) for crystal B. The resulting crystallographically determined formulas obtained for these two crystals are $[PPh_4]^+_6[Au_6Pd_6$-$(Pd_{6-x}Ni_x)Ni_{20}(CO)_{44}]^{6-}\cdot a(MeCN)\cdot b(i\text{-}Pr_2O)$, where $x = 2.90$, $a = 4.72$, $b = 1.00$ and $x = 2.10$, $a = 3.18$, $b = 1.29$ for crystals A and B, respectively. The reported nonintegral values for the solvated molecules are a consequence of their determined partial occupancies at the eight acetonitrile and two diisopropyl ether sites in the centrosymmetric triclinic unit cell coupled with

crystal-disordered solvent molecules at each site. The *composite* substitutional crystal disorder of the $(6 - x)$ Pd/x Ni atoms at the six M sites is markedly dissimilar for the seven different crystals with x ranging from 2.1 to 5.5; these differing x values correspond to a *composite six-site disorder* ranging from 65% Pd, 35% Ni to 8% Pd, 92% Ni. No evidence for any substitutional crystal disorder at the other 32-atom metal sites (i.e., 16 independent ones) in **1** was observed.

Because the three independent individual M(n) occupancies for a given crystal are reasonably similar (as was found for each of the seven crystals), we presume to a first approximation that all six crystal-disordered M sites are pseudoequivalent. This assumption results in the overall geometry of the 38-atom trimetallic core (in the crystal-averaged unit cell) ideally conforming to $D_{3d}(\bar{3}2/m)$ symmetry, in which case the six nonadjacent crystal-disordered M sites are symmetry-related by an improper $S_6(\bar{3})$ rotation axis. The entire trimetallic core has 9 octahedral, 12 trigonal bipyramidal, and 2 tetrahedral holes.

The steric disposition of the 44 carbonyl ligands consisting of 8 terminal, 30 doubly bridging, and 6 triply bridging COs also conforms to pseudo-D_{3d} symmetry (Figure 2). The eight terminal COs are each attached to one of the eight capping Ni atoms. The six triply bridging COs connect each of the six crystal-disordered M sites in a given 12-atom inner layer with two adjacent Ni atoms in the other 12-atom inner layer. These two inner layers are also connected by six doubly bridging COs, each of which edge-bridges one pair of linked Ni atoms. Each outer Pd_3 layer and its adjacent inner $Au_3M_3Ni_6$ layer are also connected by three doubly bridging COs. The other 18 doubly bridging COs form linkages between each capping Ni and a given Pd within the two Pd_3-capped triangles and a given Ni within the six $AuNi_2$-capped triangles.

Geometrical Comparison of $[Au_6Pd_6(Pd_{6-x}Ni_x)Ni_{20}$-$(CO)_{44}]^{6-}$ (1), $[Au_6Ni_{32}(CO)_{44}]^{6-}$ (2), and $[Au_6Ni_{12}(CO)_{24}]^{2-}$ (3) and Resulting Implications. Comparison of the crystal-

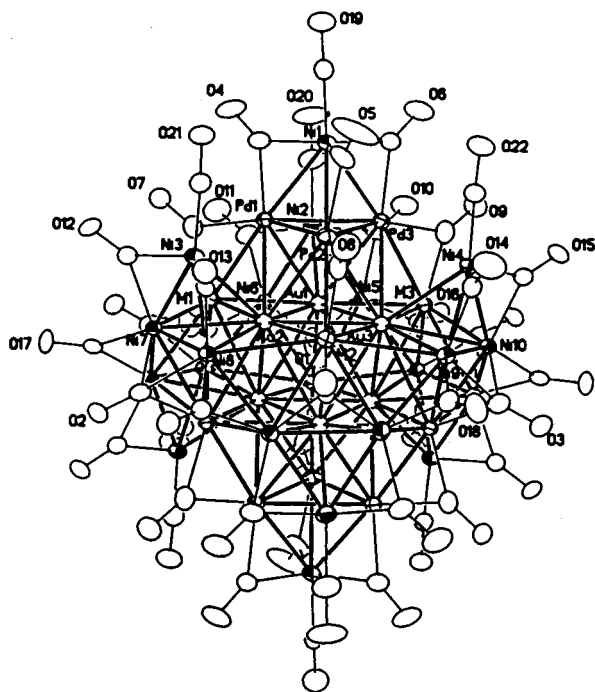$[Au_6Pd_6(Pd_{6-x}Ni_x)Ni_{20}(CO)_{44}]^{6-}$ and $[Au_6Ni_{32}(CO)_{44}]^{6-}$

J. Am. Chem. Soc., Vol. 121, No. 25, 1999 5949

Figure 2. Configuration of the entire $[Au_6Pd_6(Pd_{6-x}Ni_x)Ni_{20}(CO)_{44}]^{6-}$ (**1**) as the $[PPh_4]^+$ salt. The steric disposition of the 44 carbonyl ligands composed of 8 terminal, 30 doubly bridging, and 6 triply bridging COs also conforms to pseudotrigonal D_{3d} symmetry. **1** represents the resulting nonstoichiometric composite of all superimposed *individual* stereoisomers in the crystal-averaged unit cell of a given crystal. Anisotropic atomic displacement ellipsoids are each drawn at 50% probability.

Figure 3. View of the 38-atom Au_6Ni_{32} core in the isostructural $[Au_6Ni_{32}(CO)_{44}]^{6-}$ (**2**) in which all Pd atoms in **1** have been formally replaced by Ni atoms. Each interior Au atom of the octahedral Au_6 kernel has 12 connected metal sites corresponding to a localized hcp environment. Maximum metal-core dimensions in **1** and **2** are ca. 1.1 nm parallel and 0.8 nm perpendicular to the principal pseudo 3-fold axis.
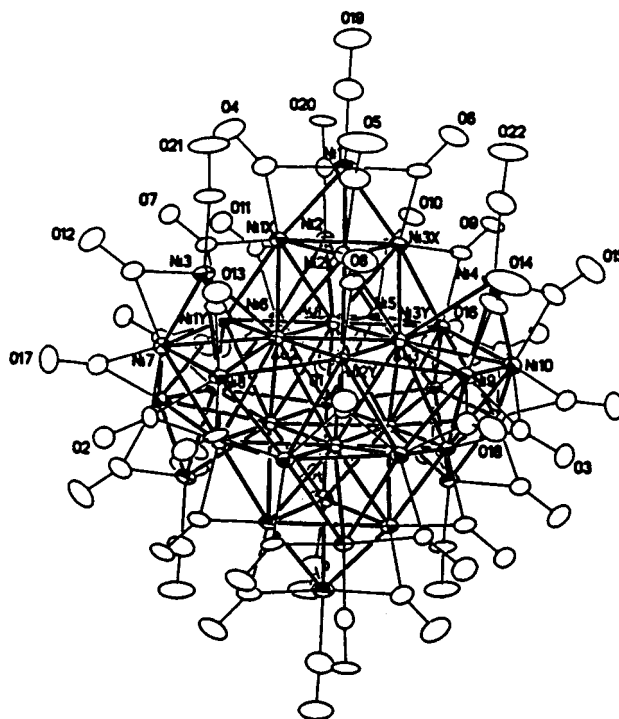
lographic unit-cell parameters for the $[PPh_4]^+$ salts of **1** and **2** indicates that their crystal structures are isomorphous. The resulting structural determination substantiates this deduction and clearly reveals that the entire geometries of **1** and **2** (Figures 3 and 4) including the connectivities of the CO ligands are closely similar. Corresponding mean distances under assumed D_{3d} symmetry are given in Table 1. Because the corresponding mean connectivities in **1** for both crystals A and B agree within 0.01 Å, only those for crystal A are presented in Table 1.

The mean of 2.88 Å for the six independent Au−Au distances in the Au_6 octahedron of **1** is analogous to that of 2.86 Å in **2** and 2.84 Å in **3**. These clusters are the only reported examples that possess a noncentered Au_6 octahedron. The possibility that the Au_6 octahedron in **3** has a second-row interstitial atom such as carbon was previously ruled out from the crystallographic analysis in accordance with the Fenske−Hall MO results and electron-counting models, providing convincing support for both its composition and structure. Likewise, each of the final difference Fourier maps in both structures of **1** in crystals A and B and that of **2** exhibited no significant electron-density residual peak at the center of the Au_6 octahedron.

The existence of $Au_6(\mu_6$-C) clusters containing a carbon-centered atom in a Au_6 octahedron was experimentally established by Schmidbaur and co-workers[16,17] from extensive physical/chemical studies of $[Au_6(PR_3)_6(\mu_6$-C)]^{2+}$ dications (R = Ph,[16] i-Pr[17]). Crystallographic investigations revealed significantly longer Au−Au edge contacts in the reformulated $[Au_6-(P\{p\text{-tol}\}_3)_6(\mu_6$-C)]^{2+}$ (3.02 Å) as the $[BPh_4]^-$ salt,[16,18] in $[Au_6(PPh_3)_6(\mu_6$-C)]^{2+}$ (3.00 Å) as the $[MeOBF_3]^-$ salt,[16] and in

Figure 4. Configuration of the isostructural $[Au_6Ni_{32}(CO)_{44}]^{6-}$ (**2**), as the $[PPh_4]^+$ salt, which has crystallographic $C_i(\bar{1})$ and pseudotrigonal D_{3d} symmetry. Anisotropic atomic displacement ellipsoids are each drawn at 50% probability.

$[Au_6(P\{i\text{-Pr}\}_3)_6(\mu_6$-C)]^{2+}$ (3.02, 3.03 Å for two independent half-cluster dications) as the $[B_3O_3F_4]^-$ salt.[17] Noteworthy is that the interstitial carbon atom in each of these $Au_6(\mu_6$-C) clusters

(16) Scherbaum, F.; Grohmann, A.; Huber, B.; Krüger, C.; Schmidbaur, H. *Angew. Chem., Int. Ed. Engl.* **1988**, *27*, 1544.

(17) Schmidbaur, H.; Brachthäuser, B.; Steigelmann, O.; Beruda, H. *Chem. Ber.* **1992**, *125*, 2705.

(18) (a) Bellon, P. L.; Manassero, M.; Naldini, L.; Sansoni, M. *J. Chem. Soc., Chem. Commun.* **1972**, 1035. (b) Bellon, P. L.; Manassero, M.; Sansoni, M. *J. Chem. Soc., Chem. Commun.* **1973**, 2423.

Table 1. Comparison of the Corresponding Means under Assumed D_{3d}^3 ($\bar{3}2/m$) Trigonal Symmetry for the Metal−Metal Connectivities (Å) in the Isostructural $[Au_6Pd_6(Pd_{6-x}Ni_x)Ni_{20}(CO)_{44}]^{6-}$ (**1**) and $[Au_6Ni_{32}(CO)_{44}]^{6-}$ (**2**)^a

metal−metal connectivities^b	$N_1{}^c$	intralayer distance^a	$N_2{}^c$	interlayer distance^a
Au−Au	6	2.89 (2.86)	6	2.88 (2.89)
Pd−Pd or Ni(X)−Ni(X)	6	2.92 (2.94)		
Ni−Ni	6	2.59 (2.59) (t)^d	18	2.42 (2.41) (d)^d
Au−Pd or Au−Ni(X)			12	2.82 (2.65)
Au−Ni	12	2.69 (2.67)	6	2.74 (2.72)
Pd−Ni or Ni(X)−Ni			6	2.66 (2.50) (d)^d
Au−M or Au−Ni(Y)	12	2.73 (2.66)	6	2.82 (2.75)
Pd−M or Ni(X)−Ni(Y)			6	2.65 (2.49) (d)^d
Ni−M or Ni−Ni(Y)	12	2.85 (2.81)	12	2.58 (2.53) (t)^d

^{a} Distances in parentheses are for **2**. ^{b} Ni(X) designates the six symmetry-equivalent Ni atoms in **2** that correspond to the six symmetry-equivalent Pd atoms in **1**, while Ni(Y) designates the six symmetry-equivalent Ni atoms in **2** that correspond to the six substitutional-disordered M atoms (viz., $Pd_{6-x}Ni_x$) in **1**. ^{c} N_1 and N_2 denote the number of symmetry-equivalent individual intralayer and interlayer metal−metal connectivities in **1** and **2**, respectively. ^{d} Symbols (d) and (t) designate metal−metal connectivities that are spanned by doubly and triply bridging COs, respectively.

gives rise to a normal electron count[19] and accounts for the significantly longer Au−Au distances. Both nonrelativistic and relativistic threoretical analyses[20,21] of these $[Au_6(PR_3)_6(\mu_6\text{-}C)]^{2+}$ dications suggest attractive tangential interactions between the Au(I) atoms with Au−Au distances of 3.0 Å; these conclusions are in accordance with spectroscopic/crystallographic evidence of Schmidbaur and co-workers[22] for the existence of attractive tangential interactions between Au(I) atoms in these and other gold compounds. The 0.1−0.2 Å shorter Au−Au distances in **1**, **2**, and **3** indicate relatively strong direct Au−Au bonding within the noncentered gold octahedron.

The mean intralayer Au−Ni connectivities of 2.69 and 2.67 Å in **1** and **2**, respectively, are significantly shorter than the corresponding mean interlayer Au−Ni connectivities of 2.74 and 2.72 Å. These values are similar to the mean Au−Ni distance of 2.69 Å in **3** and are consistent with strongly bonding Au−Ni interactions.

The six triply bridging COs in **1** and in **2** are symmetrically coordinated to the three relevant metal sites; in **1** the mean metal−μ_3-CO bond length is 2.00 Å [range, 1.983(6)−2.023(6) Å] and the mean μ_3-C−O bond length 1.17 Å, while in **2** the corresponding bond lengths are 1.98 Å [range, 1.891(8)− 2.051(8) Å] and 1.18 Å. The metal linkages of the 30 doubly bridging COs are less symmetrical; in **1** the mean metal−μ_2-CO bond length is 1.94 Å [range, 1.881(6)−2.084(7) Å] and the mean μ_2-C−O bond length 1.15 Å, while in **2** the corresponding bond lengths are 1.89 Å [range, 1.787(8)− 1.993(8) Å] and 1.17 Å. The eight terminal carbonyl ligands on the capping Ni atoms in **1** and **2** have a mean Ni−CO bond length of 1.76 Å [range, 1.758(6)−1.766(7) Å] and 1.76 Å [range, 1.753(7)−1.775(8) Å], respectively, and a corresponding mean C−O bond length of 1.14 and 1.15 Å, respectively.

Atomic Site Preferences in Heterometallic Systems. (a) General Comments. The structural preference and distribution

of different metal atoms in mixed-metal clusters may be considered as a manifestation of differences in the bond capabilities of the different metal constituents. A recent comprehensive review by Miller[23] examines this "coloring problem" in extented and intermetallic solids. It also illustrates how second moment scaling techniques and the structural difference theorem have provided good estimates of the structural energy differences for different atomic arrangements. These calculations have been highly successful in predicting structure/composition/property relationships in many binary intermetallic compounds.

In another recent report, Teo et al.[24] showed that a simple quantitative model based solely on calculated relative metal−metal bond energies successfully predicts the atomic site preferences of the different metal atoms found in their remarkable vertex-sharing centered polyicosahedral series of bimetallic (Au−Ag) and trimetallic (Au−Ag−M; M = Ni, Pd, Pt) clusters possessing phosphine/halide ligands.[25] They pointed out that their model,[26] which provides a relative measure of the strengths of metal−metal bonds in a mixed-metal cluster and hence the relative energetic stabilities of various stereoisomers, can be applied to other transition metal clusters or intermetallic systems where differences in metal−metal bonding are dominant relative to differences in metal−ligand bonding.

(b) Analysis of the Segregated Au/Ni, Pd Metal Core in $[Au_6Pd_6(Pd_{6-x}Ni_x)Ni_{20}(CO)_{44}]^{6-}$ (1). 1 is analogous to $[Au_6Ni_{12}(CO)_{24}]^{2-}$ (**3**) in being a molecular analogue of the chemisorption-induced aggregation (CIA) model that was experimentally formulated from surface-science composition studies[27] for bimetallic systems including group 10 (Ni, Pd, Pt) and group

(19) (a) Mingos, D. M. P. *J. Chem. Soc., Dalton Trans.* **1976**, 1163. (b) Mingos, D. M. P. *Nature (London)* **1990**, *345*, 113.

(20) Mingos, D. M. P.; Kanters, R. P. F. *J. Organomet. Chem.* **1990**, *384*, 405.

(21) (a) Rösch, N.; Görling, A.; Ellis, D. E.; Schmidbaur, H. *Angew. Chem., Int. Ed. Engl.* **1989**, *28*, 1357. (b) Görling, A.; Rösch, N.; Ellis, D. E.; Schmidbaur, H. *Inorg. Chem.* **1991**, *30*, 3986.

(22) (a) Schmidbaur, H. *Gold Bull.* **1990**, *23*, 11. (b) Schmidbaur, H.; Brachthäuser, B.; Steigelmann, O. *Angew. Chem., Int. Ed. Engl.* **1991**, *30*, 1357. (c) Steigelmann, O.; Bissinger, P.; Schmidbaur, H. *Angew. Chem., Int. Ed. Engl.* **1990**, *29*, 1399. (d) Grohmann, A.; Riede, J.; Schmidbaur, H. *Nature* **1990**, *345*, 140. (e) Scherbaum, F.; Grohmann, A.; Müller, G.; Schmidbaur, H. *Angew. Chem., Int. Ed. Engl.* **1989**, *28*, 463. (f) Schmidbaur, H.; Graf, W.; Müller, G. *Angew. Chem., Int. Ed. Engl.* **1988**, *27*, 417. (g) Schmidbaur, H.; Scherbaum, F.; Huber, B.; Müller, G. *Angew. Chem., Int. Ed. Engl.* **1988**, *27*, 419. (h) Schmidbaur, H.; Hartmann, C.; Reber, G.; Müller, G. *Angew. Chem., Int. Ed. Engl.* **1987**, *26*, 1146. (i) Nakamoto, M.; Hiller, W.; Schmidbaur, H. *Chem. Ber.* **1993**, *126*, 605.

(23) Miller, G. J. *Eur. J. Inorg. Chem.* **1998**, 523 and references therein.

(24) Teo, B. K.; Strizhev, A.; Elber, R.; Zhang, H. *Inorg. Chem.* **1998**, *37*, 2482 and references therein.

(25) (a) Teo, B. K.; Zhang, H.; Shi, X. *Inorg. Chem.* **1994**, *33*, 4086. (b) Teo, B. K.; Zhang, H. *Coord. Chem. Rev.* **1995**, *143*, 611. (c) Zhang, H.; Teo, B. K. *Inorg. Chim. Acta* **1997**, *265*, 213.

(26) The Teo model[24] assumes that metal−metal bonding in a heterometallic stereoisomer is composed of two major components, namely, covalent and ionic contributions, which are modeled in the bond energy calculations by use of cohesive energies and electronegativities, respectively. The distance dependence of the metallic bonding energy was modeled by the Leonard-Jones potential. From their calculated bond energies, Teo et al.[24] formulated two site-preference rules. The strong-bond rule, which arises from the covalent contribution, states that stereoisomers having a higher number of "strong bonds" tend to be more stable; this implies that metals that are capable of forming strong metal−metal bonds tend to occupy interstitial or high-connectivity positions. The hetero-bond rule, which originates from the ionic character of a heterometallic bond, tends to maximize the number of such bonds (at the expense of homonuclear ones), in which case *like* metal atoms tend not to be nearest neighbors. Stereoisomers with higher total metallic bond energies are then presumed to be thermodynamically more stable (provided that metal−ligand bonding effects can be ignored).

[Au₆Pd₆(Pd₆₋ₓNiₓ)Ni₂₀(CO)₄₄]⁶⁻ and [Au₆Ni₃₂(CO)₄₄]⁶⁻

J. Am. Chem. Soc., Vol. 121, No. 25, 1999 5951

11 (Cu, Ag, Au) atoms. The normal surface-enrichment composition rule for bimetallic particles (under ultrahigh vaccuum) is that the metal component with the lower heat of sublimation (normally weaker metal−metal interactions) should concentrate at the surface in order to lower the surface tension. However, the thermodynamic-based CIA model allows the surface-enriched component to be reversed if an absorbate gas binds strongly and selectively to the other metal component with the higher heat of sublimation. Because gold has a lower sublimation energy than a group 10 metal, gold normally should be concentrated at the surface in the absence of an absorbate (ligand) preferentially coordinated to a group 10 metal. Thus, the occurrence in **1** and **3** of a segregated Au₆ kernel surrounded by group 10 surface atoms (instead of a Ni, Pd-rich inner core in **1** with surface gold atoms) is due to the selective strong coordination of the carbonyls to the Ni, Pd atoms. The much stronger (Pd, Ni)−CO bonding interactions in **1** simply predominate over the opposing site preference effects of the metal−metal bond energies.

Analogous general conclusions concerning site preference effects in naked and ligated heterometallic clusters were reported by Mingos and Zhenyard[28] on the basis of their extensive analysis of a large number of mixed-metal clusters via MO perturbation theory.

(c) Analysis of the Substitutional Pd/Ni Crystal Disorder (Coloring Problem) in [Au₆Pd₆(Pd₆₋ₓNiₓ)Ni₂₀(CO)₄₄]⁶⁻ (1) and Resulting Implications. A qualitative stereochemical analysis of this trimetallic cluster provides an explanation why the Pd/Ni substitutional crystal disorder in **1** occurs only at the six nonadjacent pseudoequivalent M sites (under assumed D_{3d} symmetry). The preferential existence of only Ni atoms at the eight capping metal sites in **1** is clearly due to the composite terminal/bridging COs forming much stronger bonding interac-

tions with Ni than with Pd. Convincing evidence for the relative weakness of terminal Pd−CO bonds is that only a few Pd complexes (and clusters) possessing terminal carbonyl ligands are known;[9,29,30] of these, a considerable number are not thermally stable and undergo decarbonylation.

The presence of *only* Pd atoms at the six pseudoequivalent sites in the two outer triangular Pd₃ layers and *only* Ni atoms at the 12 pseudoequivalent sites in the two inner Au₃M₃Ni₆ layers but substitutional Pd /Ni crystal disorder at the 6 M sites can be attributed primarily to the extent of dissimilar metal−metal bonding interactions that are modulated by stronger metal−CO bonding interactions. The relative strengths of such interactions in **1** critically depend on interatomic distances within the distorted close-packed metal-core geometry that are markedly influenced by atom-size differences[31] and bond-shortening effects of the bridging carbonyl ligands. Thus, the large metal−metal mean distance of 2.92 Å found in the Pd₃ triangles exclusively favors Pd over Ni in that the less-contracted valence Pd AOs[24] would no doubt form much stronger metal−metal connectivities at such a long distance. Conversely, the occurrence of only Ni atoms at the 12 symmetry-related sites in the two Au₃M₃Ni₆ layers is ascribed to CO-bridged Ni−Ni connectivities being considerably stronger (due mainly to Ni−CO bonding interactions) at the observed short interlayer distances (mean, 2.42 Å). In contrast, the six M sites form intermediate mean distances to Au (2.73, 2.82 Å), Pd (2.65 Å), and Ni (2.85, 2.58 Å); hence, any site preference effects due to differences in combined metal−metal and metal−CO bonding are deemed not to be nearly as influential, in accordance with substitutional Pd/Ni crystal disorder being found *only* at the six M sites for a given crystal. In other words, the Pd/Ni crystal disorder that occurs solely at the M sites arises because of insignificant stabilization-energy differences in the combined bond and site energies.

Table 1 provides a comparison of mean distances under pseudo-D_{3d} symmetry for the corresponding metal−metal connectivities in **1** and **2**. The formal replacement of the six symmetry-equivalent Pd atoms in **1** by Ni(X) atoms in **2** is of particular relevance in providing additional evidence why Pd atoms exclusively occupy these six sites in **1**. In **2** the smaller Ni(X) atoms result in a 0.02 Å increase (instead of a decrease) in the mean intralayer Ni(X)−Ni(X) distance. This mean of 2.94 Å is indicative of very *weak* Ni(X)−Ni(X) bonding in **2**. At such a long distance, the corresponding Pd−Pd bonding in **1** must be much stronger (vide supra). This large difference in metal−metal bond energy is presumed to be a dominant stabilization-energy factor in accounting for the exclusive occupancy by Pd atoms of its six symmetry-equivalent sites in **1**.

Formal replacement of the Pd atoms at the crystal-disordered M sites by Ni atoms (designated in **2** as Ni(Y) sites) expectedly causes significantly shorter mean distances (Table 1) of the Pd−Ni, Au−M, Pd−M, and Ni−M connectivities relative to those

(27) (a) Bouwman, R.; Sachtler, W. M. H. *J. Catal.* **1970**, *19*, 127. (b) Bouwman, R.; Lippits, G. J. M.; Sachtler, W. M. H. *J. Catal.* **1972**, *25*, 350. (c) Williams, F. L.; Boudart, M. *J. Catal.* **1973**, *30*, 438. (d) Sinfelt, J. H. *Acc. Chem. Res.* **1987**, *20*, 134 and references therein.

(28) Mingos, D. M. P.; Zhenyang, L. *Comments Inorg. Chem.* **1989**, *9*, 95.

(29) (a) Pd(CO)ₙ (n = 1−4; matrix isolation at 4.2−10 K): Kiindig, E. P.; McIntosh, D.; Moskovits, M.; Ozin, G. A. *J. Am. Chem. Soc.* **1973**, *95*, 7234. Darling, J. H.; Ogden, J. S. *Inorg. Chem.* **1972**, *11*, 666. (b) Pd-(CO)₃(PPh₃): Whyman, R. *J. Organomet. Chem.* **1973**, *63*, 467 and references therein. (c) Pd(CO)(triphos) (triphos = MeC(CH₂PPh₂)₃), Pd-(CO)(NP₃) (NP₃ = N(CH₂PPh₂)₃): Greven, J.; Kalck, Ph.; Daran, J. C.; Vaissermann, J.; Bianchini, C. *Inorg. Chem.* **1993**, *32*, 4965. (d) [PdX₃-(CO)]⁻: (X = Cl, Br, I): Browning, J.; Goggin, P. L.; Goodfellow, R. J.; Norton, M. G.; Rattray, J. M.; Taylor, B. F.; Mink, J. *J. Chem. Soc., Dalton Trans.* **1977**, 2061. Andreini, B. P.; Belli Dell'Amico, D.; Calderazzo, F.; Venturi, M. G.; Pellizzi, G. *J. Organomet. Chem.* **1988**, *354*, 369. (e) *cis*-Pd(CO)₂(SO₃F)₂: Wang, C.; Willner, H.; Bodenbinder, M.; Batchelor, R. J.; Einstein, F. W. B.; Aubke, F. *Inorg. Chem.* **1994**, *33*, 3521. (f) [Pd-(CO)₄]²⁺: Hwang, G.; Wang, C.; Aubke, F.; Willner, H.; Bodenbinder, M. *Can. J. Chem.* **1993**, *71*, 1532 and references therein. Hwang, G.; Bodenbinder, M.; Willner, H.; Aubke, F. *Inorg. Chem.* **1993**, *32*, 4667. (g) *cis*-Pd(CO)₂(C₆X₅)₂ (X = Cl, F): Usón, R.; Forniés, J.; Tomás, M.; Menjón, B. *Organometallics* **1985**, *4*, 1912. (h) Pd(η³-C₄H₇)(SnCl₃)(CO): Grassi, M.; Meille, S. V.; Musco, A.; Pontellini, R.; Sironi, A. *J. Chem. Soc., Dalton Trans.* **1989**, 615. (i) [Pd(R)Cl₂(CO)]⁻ (R = C₆H₃Me-2, NO₂-6; R = C₆H₂-(NO₂)₃-2,4,6): Vicente, J.; Arcas, A.; Borrachero, M. V.; Tiripicchio, A.; Camellini, T. *Organometallics* **1991**, *10*, 3873. (j) Pd₂(CO)₂Cl₂(μ₂-Cl)₂: Belli Dell'Amico, D.; Calderazzo, F.; Veracinni, C. A.; Zandona, N. *Inorg. Chem.* **1984**, *23*, 3030 and references therein. (k) Pd₂(CO)₂Br₂(μ₂-Br)₂: Andreini, B. P.; Belli Dell'Amico, D.; Calderazzo, F.; Venturi, M. G.; Pelizzi, G. *J. Organomet. Chem.* **1988**, *354*, 369. (l) Pd₂(CO)₄(μ₂-Cl)₂: Soriano-Garcia, M.; Rosas, N.; Gomez-Lara, J.; Toscano, R. A. *Acta Crystallogr.* **1987**, *C43*, 1679. (m) [Pd₂(CO)₂(PHBuᵗ₂)₂(μ₂-PBuᵗ₂)]⁺: Leoni, P.; Pasquali, M.; Sommovigo, M.; Laschi, F.; Zanello, P.; Albinati, A.; Lianza, F.; Pregosin, P. S.; Rüegger, H. *Organometallics* **1993**, *12*, 1702. (n) Pd₃(CO)₂Cl(μ₂-PBuᵗ₂)₃: Arif, A. M.; Heaton, D. E.; Jones, R. A.; Nunn, C. M. *Inorg. Chem.* **1987**, *26*, 4228. (o) Pd₃(CO)₃{μ₂-M′(NR₂)₂}₃ (M′ = Ge, Sn; R = SiMe₃): Campbell, G. K.; Hitchcock, P. B.; Lappert, M. F.; Misra, M. C. *J. Organomet. Chem.* **1985**, *289*, C1.

(30) (a) Stromnova, T. A.; Moiseev, I. I. *Russ. Chem. Rev.* **1998**, *67*, 485. (b) Lee, S. M.; Wong, W. T. *J. Cluster Sci.* **1998**, *9*, 417. (c) Mingos, D. M. P.; Vilar, R. *J. Organomet. Chem.* **1998**, *557*, 131. (d) Structure Index, Ed: Bruce, M. I. In *Comprehensive Organometallic Chemistry II*; Abel, E. W., Stone, F. G. A., Wilkinson, G., Eds.; Elsevier Science Inc.: Tarrytown, NY, 1995; Vol. 13, pp 728−752. (e) Dixon, K. R.; Dixon, A. C. In *Comprehensive Organometallic Chemistry II*; Abel, E. W., Stone, F. G. A., Wilkinson, G., Eds.; Elsevier Science Inc.: Tarrytown, NY, 1995; Vol. 9. *Ibid.* Puddephatt, R. J., Ed.; pp 193−223. (f) Burrows, A. D.; Mingos, D. M. P. *Transition Met. Chem.* **1993**, *18*, 129. (g) Kharas, K. C. C.; Dahl, L. F. *Adv. Chem. Phys.* **1988**, *70* (Part 2), 1. (h) Eremenko, N. K.; Mednikov, E. G.; Kurasov, S. S. *Russ. Chem. Rev.* **1985**, 394.

(31) Covalent radii are Ni (1.20 Å), Pd (1.31 Å), and Au (1.43 Å): Porterfield, W. W. *Inorganic Chemistry: A Unified Approach*; Addison-Wesley: Reading, MA, 1984; p 168.

of the corresponding Ni(X)−Ni, Au−Ni(Y), Ni(X)−Ni(Y), and Ni−Ni(Y) connectivities, respectively. It is impossible to assess qualitatively why substitutional Pd/Ni crystal disorder occurs at the M sites in **1**; one can only generalize that it arises because the resulting composite metal−metal and metal−CO bond energies (and hence the overall relative energy stabilities) are *not* significantly different for each individual stereoisomer (i.e., **1** represents the resulting nonstoichiometric composite of all superimposed individual stereoisomers in the crystal-averaged unit cell of a given crystal).

Application of Electron-Counting Models to [Au$_6$Pd$_6$-(Pd$_{6-x}$Ni$_x$)Ni$_{20}$(CO)$_{44}$]$^{6-}$ (1) and [Au$_6$Ni$_{32}$(CO)$_{44}$]$^{6-}$ (2) and Resulting Implications. The observed number of metal cluster valence electrons (CVEs) in the Au$_6$Pd$_6$(Pd$_{6-x}$Ni$_x$)Ni$_{20}$ core of **1** and in the Au$_6$Ni$_{32}$ core of **2** is 480 (i.e., 6×11 (Au) + 32×10 (Pd,Ni) + 44×2 (CO) + 6 (charge) = 480). In order for the Au$_6$ kernel in **1** to be completely encapsulated by a convex metal polyhedron, we initially assumed that the six AuNi$_2$-capped Ni atoms are also (edge-bridged)-linked to the two Pd$_3$ triangles as part of a highly distorted fragment of a close-packed metal lattice. A major consequence of this assumed close-packed metal arrangement (even at nonbonding contacts) is that the Mingos model,[32] which presumes that radial interactions dominate in a close-packed metal cluster, can then be utilized. The total valence electron count given by $\Delta_i + 12n_s$, where Δ_i is the central fragment count (viz., 86 for the Au$_6$ octahedron) and n_s is the number of surface atoms (viz., 32), is 470. The topological shell-model rule given by the Teo/Zhang model[33] for close-packed metal clusters is $T_n = 6G_n + K$, where T_n denotes the total number of topological electron pairs, G_n the total number of metal atoms in a close-packed cluster, and $K = 7$ for a completely encapsulated Au$_6$ octahedron. Consequently, the calculated electron count is $N = 2T_n = 2(6G_n + K) = 2(6 \times 38 + 7) = 470$. The calculated number of 470 electrons for the CVEs obtained from the use of either the Mingos model[32] or the Teo/Zhang model[33] for close-packed metal clusters is 10 electrons less than the observed number. An explanation accounting for this large electron-count difference is that our assumption that the entire metal core of **1** conforms to a *close-packed* polyhedron is *not* valid.

We suggest that both models, which only apply to close-packed polyhedral metal clusters, are *not* applicable because the extra electrons (in the observed count) presumably form antibonding Ni(capping)−Pd interactions; this hypothesis is consistent with the six independent edge-bridged Ni(capping)−Pd distances, which range from 3.18 to 3.54 Å in **1**, being essentially nonbonding.[34] Actual linkages at shorter bonding Ni-(capping)−Pd distances to give a close-packed cluster would presumably result in loss of the terminal CO attached to each of the six capping Ni atoms, such that the resulting observed electron count of 468 (instead of 480) would then be compatible with the calculated one of 470. Figure 1 reveals that the considerable tilting of the six AuNi$_2$-capped Ni atoms away from the two outer Pd$_3$ layers in **1** may be attributed to the much

larger size of the Au atom relative to that of the two Ni atoms.[31] Thus, these six capping Ni atoms are geometrically prevented from being part of the highly distorted hcp Au$_6$M$_6$Ni$_{12}$Pd$_6$ fragment.

Further Synthetic Investigations. The redox reactions that give rise to the noncentered Au$_6$ octahedron in **1**, **2**, and **3** require cleavage of the PPh$_3$ ligand from each Au atom of the Au-(PPh$_3$)Cl precursor. This Au−PPh$_3$ bond scission is highly unusual and a rare exception in countless metal cluster reactions involving Au(PPh$_3$)X reagents (X = halide, nitrate). This bond cleavage is apparently associated with a marked weakening of the Au−P bond upon reduction of the Au(I) by the strong reducing agent, [Ni$_6$(CO)$_{12}$]$^{2-}$.

The characterization from X-ray diffraction analyses of the microscopic nature of the crystalline substitution disorder in [Au$_6$Pd$_6$(Pd$_{6-x}$Ni$_x$)Ni$_{20}$(CO)$_{44}$]$^{6-}$ (**1**) stimulated further synthetic work involving the use of different palladium compounds as starting materials. This research involved reactions of [Ni$_6$-(CO)$_{12}$]$^{2-}$ with DMSO containing similar mole ratios of Au-(PPh$_3$)Cl with each of the following palladium compounds: Pd-(OAc)$_2$, Pd(CH$_3$CN)$_2$Cl$_2$, Pd(CH$_3$CN)$_4$(BF$_4$)$_2$, PdCl$_2$, and Pd$_2$-(dba)$_3$. Reactions with each of these palladium compounds produced **1** in similar yields. When Pd(PPh$_3$)$_2$Cl$_2$ was used, the reaction did not produce **1** but instead gave rise to other as yet uncharacterized products.

Efforts to prepare two other structurally analogous stoichiometric hypothetical analogues of **1**, namely, [Au$_6$Pd$_6$Ni$_{26}$(CO)$_{44}$]$^{6-}$ and [Au$_6$Pd$_{12}$Ni$_{20}$(CO)$_{44}$]$^{6-}$, by systematic variations of the mole ratios of [Ni$_6$(CO)$_{12}$]$^{2-}$/Pd(OAc)$_2$ used in the reactions were unsuccessful. For the same purpose, a mixture of Ni(OAc)$_2$ and Pd(OAc)$_2$ was used to react with [Ni$_6$(CO)$_{12}$]$^{2-}$ and Au(PPh$_3$)-Cl. An excellent yield of **1** was obtained in both the acetone and acetonitrile extracts. However, X-ray diffraction analyses revealed the existence of the substitutional Pd/Ni crystal disorder only at the six S_6-related metal sites.

Fortunately, the isolated crystals of **2**, obtained from the reaction of Ni(OAc)$_2$ with [Ni$_6$(CO)$_{12}$]$^{2-}$ and Au(PPh$_3$)Cl, enabled both X-ray diffraction and IR measurements to be carried out. In light of **2** being isostructural with **1**, it is not surprising that their IR spectra are virtually identical in the carbonyl region. Further work is ongoing to obtain appropriate reaction conditions, from which **2** and the two other Au−Ni clusters can be separated from one another in solution and isolated in sufficient quantities for detailed physical/chemical characterization. The results of this research will be reported elsewhere.

Supporting Information Available: Tables listing crystallographic data for crystals A and B of **1** and for **2** (PDF). This material is available free of charge via the Internet at http://pubs.acs.org.

(32) (a) Mingos, D. M. P. *J. Chem. Soc., Chem. Commun.* **1985**, 1352. (b) Mingos, D. M. P.; Zhenyang, L. *J. Chem. Soc., Dalton Trans.* **1988**, 1657.

(33) (a) Teo, B. K.; Zhang, H.; Kean, Y.; Dang, H.; Shi, X. *J. Chem. Phys.* **1993**, *99*, 2929. (b) Teo, B. K.; Zhang, H. *Polyhedron* **1990**, *9*, 1985. (c) Teo, B. K.; Sloane, N. J. A. *Inorg. Chem.* **1986**, *25*, 2315.

(34) In **2** the corresponding six independent Ni(capping)−Ni(X) distances vary from 3.1 to 3.5 Å (mean, 3.3 Å).

JA982637C